Visualization of the Resistance Spot Welding Process in the Production Line

A proposed sensor system provides visualization and optimization of the resistance spot welding process during production

BY J. HEß, T. KERN, W. KRIEGL AND M. SCHWEIZER

ABSTRACT. A system is presented that allows the visualization of the whole welding process. Factors that can lead to bad welds can be monitored. Methods to optimize the welding process are outlined and a possible "on-line control" is discussed. In addition, schemes are presented for the analysis of the welding process to identify defects in the welding equipment that will cause faulty welds.

Introduction

Resistance spot welding (RSW) is the most common method of joining metal sheets. Although widely used for industrial applications, there currently exists no commonly accepted control or visualization system for this process in the production line. Despite the fact that various process parameters such as pressure applied to the cylinder, the flow of cooling water and the welding current can be monitored, faulty spot welds still occur. In the automotive industry, for instance, considerable efforts are made to ensure the quality of spot welds by manual inspection and reworking. The development of a system that provides an on-line control during production or even points out the factors that can cause faulty welds is desirable.

A great deal of theoretical and experimental scientific work has been done on the spot welding process. Although the general features of the nugget formation are well understood (Refs. 1, 2), there are about 40 factors according to Quanz (Ref. 3) that could reduce the quality of a spot weld and yield, at the worst, faulty welds. In many cases, the mechanisms leading to these failures are not well understood. Hence, one major aim of our research work is the identification, understanding and prevention of those mechanisms. This is best done by examining a quantity directly correlated with the formation of the nugget.

A number of measurement techniques have been developed in recent years that claim to correlate well with weld quality. Weber, *et al.* (Refs. 4, 5), studied the dynamic resistance between the electrode caps while a spot weld was formed. A detailed study of electrode force measurements has been undertaken by Dorn, *et al.* (Ref. 6). Stiebel, *et al.* (Ref. 7), presented a paper in which electrode displacement was studied. Various other articles have been published about the application of ultrasonic techniques (Refs. 8, 9). A detailed overview of the methods for welding control has been worked out by Polrolniczak (Ref. 10). Although the results of these investigations allow classification of spot welds in the laboratory, none of these has been widely introduced into the production line.

It has been pointed out by Tsai, *et al.* (Ref. 11), that the electrode cap displacement caused by the thermal expansion of the molten material shows a good correlation to weld quality as it is directly caused by the formation of the nugget. Since this quantity provides insight into the welding process, it seems to fulfill all the conditions necessary to establish a control and visualization system for spot welds. Therefore, a method has been developed to determine electrode cap displacement indirectly by measuring the deflection of the electrode arm. This method enables the user to control spot welding with suitable welding tongs and allows the visualization of certain defects of the welding equipment in the production line, as well as in the laboratory.

KEY WORDS

Electrode Force
Resistance Spot Welding
Visualization of Welding Process
Weld Nugget
Welding Sensor

The Measurement Equipment

Generally, the measurements of electrode cap movement are not practical in the production line; however, deflection of the electrode arm together with the movement of the piston reveals the same mechanical information. Assuming that the piston movement is inhibited due to static friction during the welding process, we may restrict the following discussions to the electrode arm deflection when the welding gun grasps the workpiece and is affected by the thermal expansion of the spot weld.

The deformation $\varepsilon_{el}(x)$ (measured in units of strain) applied by the piston to the electrode arm may be calculated by the elementary theory of the deflection beam as follows:

$$\varepsilon_{el}(x) = \frac{F_{el} \cdot (L_0 - x) \cdot r}{E \cdot I_q} \quad (1)$$

where F_{el} is the electrode force applied by the piston, x is the distance between the bearings of the tongs and the position of the sensor, I_q is the geometrical moment of inertia of the electrode arm, E is Young's modulus of elasticity, L_0 is the length and r is the radius of the electrode arm — Fig. 1.

J. HEß is with Zimmer AG, Frankfurt, Germany. T. KERN is with F. H. Brandenburg, Brandeburg, Germany. W. KRIEGL is with Sensor Instruments GmbH, Thurmansbang, Germany. M. SCHWEIZER is with Robert Bosch GmbH, Stuttgart, Germany.

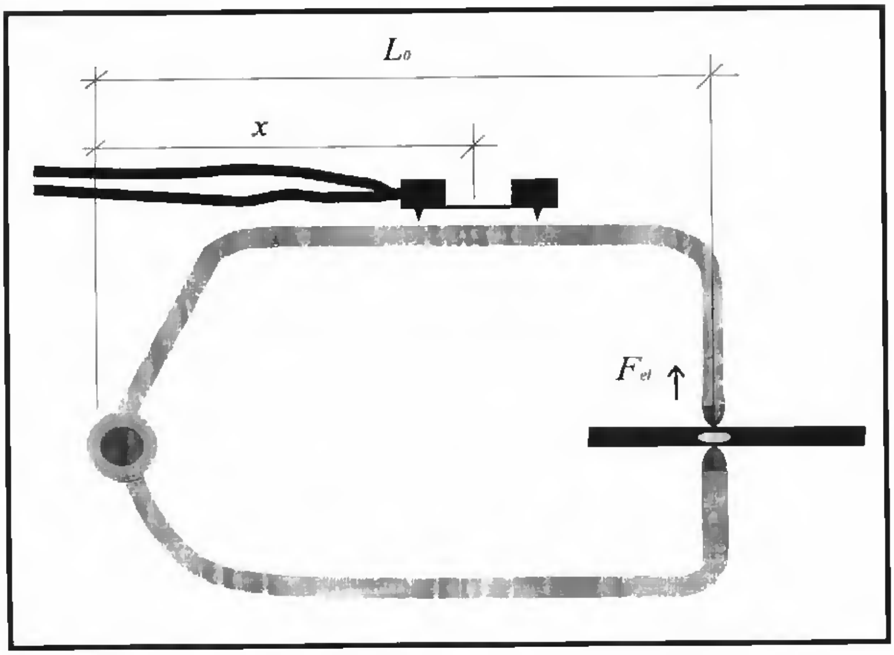

Fig. 1 — Application of the sensor on a welding tong.

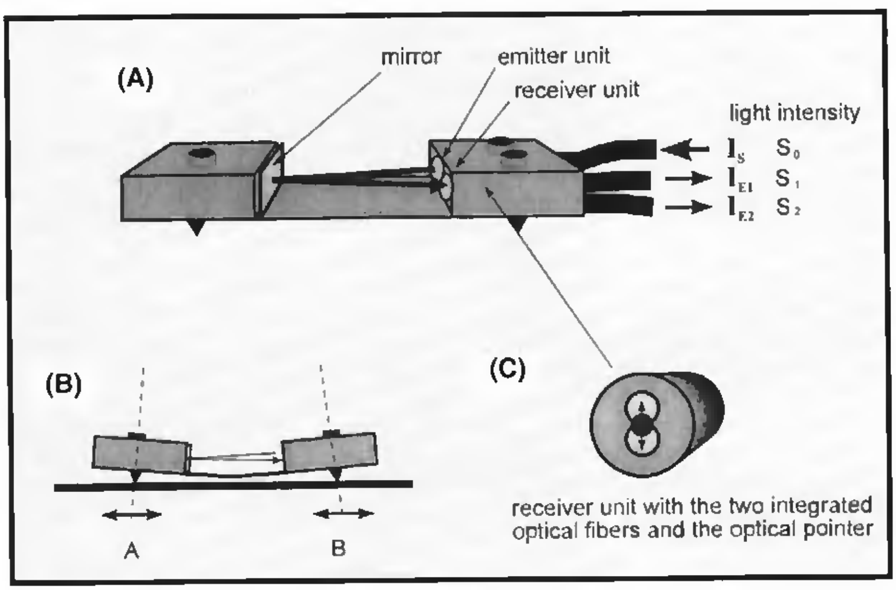

Fig. 2 — Operation principle of the expansion sensor applied to the electrode arm. A — Complete setup of the sensor; B — the sensor application at the electrode arm; C — the receiver unit with the optical pointer.

The thermal expansion of the spot weld is approximately $\delta\xi_{th} = 100$ pm. The correlation between the thermal expansion and the quasi-force, F_q, which would be necessary to induce the same deformation of the electrode arm, may be calculated as

$$\delta\xi_{th} = \frac{F_q \cdot L_0^3}{3 \cdot E \cdot I_q}. \qquad (2)$$

The corresponding deformation ε_{th} of the electrode arm x is

$$\varepsilon_{th}(x) = 3 \cdot \frac{\delta\xi_{th} \cdot (L_0 - x) \cdot r}{L_0^3}. \qquad (3)$$

The ratio of both deformations is given by

$$\frac{\varepsilon_{th}(x)}{\varepsilon_{el}(x)} = \frac{3 \cdot \delta\xi_{th} \cdot E\, I_q}{F_{el} \cdot L_0^3}. \qquad (4)$$

For a typical electrode arm with $L_0 =$ 400 mm, its radius $r = 20$ mm, the material copper with $E = 1.23 \times 10^{11}$ N/m^2, $I_q = 12.6 \times 10^{-8}$ m^4 and $F_{el} = 2.2$ kN, the ratio is $\varepsilon_{th}/\varepsilon_{el} \approx 3\%$.

To determine the deflection of the electrode arm with sufficient accuracy, a sensor of high sensitivity is needed. On the other hand, a strong, alternating magnetic field generated by the welding current is present during the welding time. As distortions by induced voltages cannot be excluded with conventional expansion sensors (e.g., strain gauges), an optical sensor working on the light pointer principle was developed. For the same reason, the information transfer between the sensor and its control unit must be realized via optical cables.

The sensor consists of a nonmagnetic base plate with integrated optical elements, and exhibits a section where bending is intended. The sensor is fixed on the electrode arm at points A and B — Fig. 2. The bending of the electrode arm leads to a displacement δx of A and B and to a dilatation and a bending of the sensor. For a distance of 30 mm between A and B, this displacement, δx, can be estimated as $\delta x \approx 50$ pm under load.

The operation principle of the sensor is illustrated in Fig. 2. The light beam from the emitter unit is reflected by a mirror at the other end of the bending section. The bending of the electrode arm leads to a tilting of the mirror and deflection of the optical pointer. The light beam is focused onto the receiver unit, which displays the ends of two optical fibers, as shown in Fig. 2. The light flux through the lower and upper fiber depends on the tilt angle of the mirror. An expansion of the sensor of δx deflects the light beam from the center position between the two optical fibers toward the lower fiber. The registered light intensity transmitted by the lower fiber s_1 increases and the intensity s_2 of the upper fiber decreases by about the same amount. To minimize the influence of different attenuation parameters of the two optical fibers and their change caused by aging, the value

$$q = \frac{s_1 - \beta \cdot s_2}{s_1 + \beta \cdot s_2} \qquad (5)$$

is calculated by the control unit. β is a fitting parameter that compensates for the different attenuation parameters of the optical fibers. This parameter β needs occasional adjustment.

The sensor signal q is not exactly linear in the displacement δx, due to the nonlinear geometrical and optical characteristics of the light pointer and the receiver unit — Fig. 2. However, the linearity between both quantities is sufficient over the range of interest in all practical applications as shown in Fig. 3, where the sensor signal q is plotted vs. the displacement δx. No distortions caused by the welding current are visible on the signals.

Evaluation of the Data

Given the considerations made in the preceding section, a sharp increase of the signal q after the closing of the tongs followed by a plateau is expected. During the welding time, a small peak — referred to as *welding peak* — is superimposed onto the electrode force. This additional force originates from the thermal expansion of the nugget.

In resistance spot welding, three different categories of spots are observed. As shown in Fig. 4, three electrode force curves over a complete welding process with increasing currents represent these categories:

1) *Spot Weld with Insufficient Load Capacity:* If the welding current is too low or electrode caps are worn, no nugget is produced; or if produced, the nugget is too small. Consequently, the thermal expansion of the nugget and the welding peak are small.

2) *Spot Weld with Sufficient Load Capacity:* For the formation of a spot weld with enough load capacity, more energy is needed. This leads to a larger thermal expansion resulting in a larger welding peak.

3) *Spatters:* The expansion of the nugget terminates in the expulsion of molten material. Spatters generally occur if the welding current is too high or the electrode force is too small. The expulsion of molten material is accompanied by a quick motion of the electrode caps toward each other, which is visible in the signal as a sudden decrease in the electrode force.

All welds were performed with 1-mm-thick galvanized steel sheets (as are widely used in the automotive industry). The electrode caps used in these experiments have a contact area of a

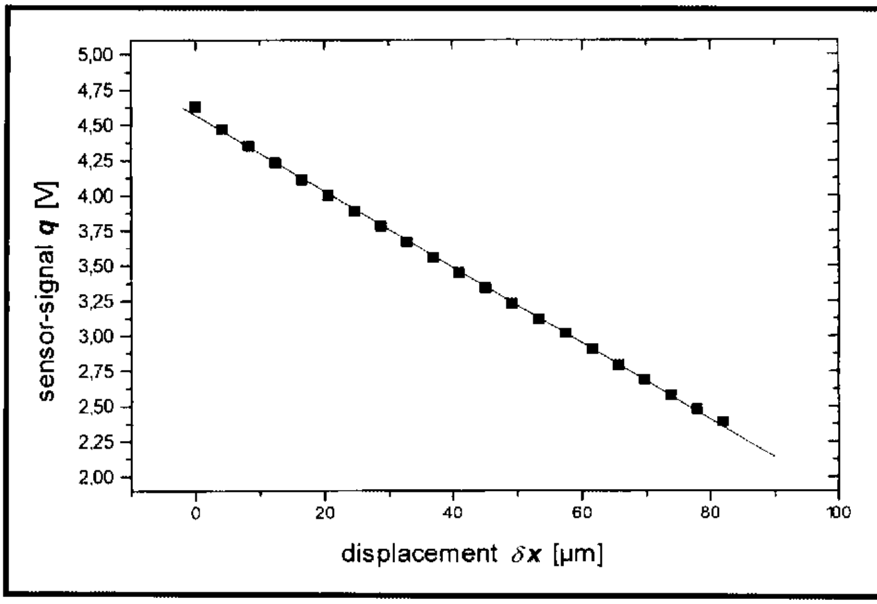

Fig. 3 — The signal height q vs. the displacement δx.

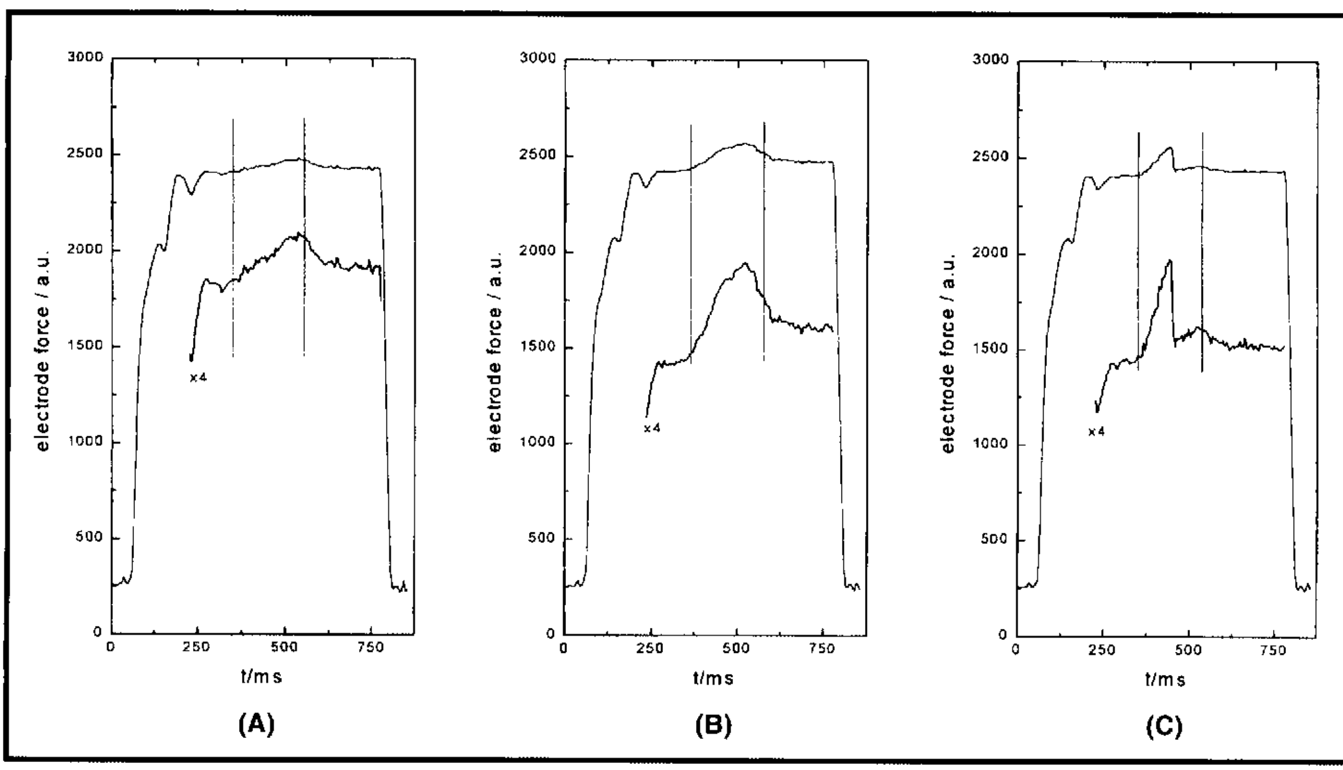

Fig. 4 — Electrode force curves for different welding conditions for the following: A — Spot weld with insufficient load capacity; B — spot weld with sufficient load capacity; C — spatters. The fourfold amplified signal shifted by an appropriate offset value is displayed below the sensor signal.

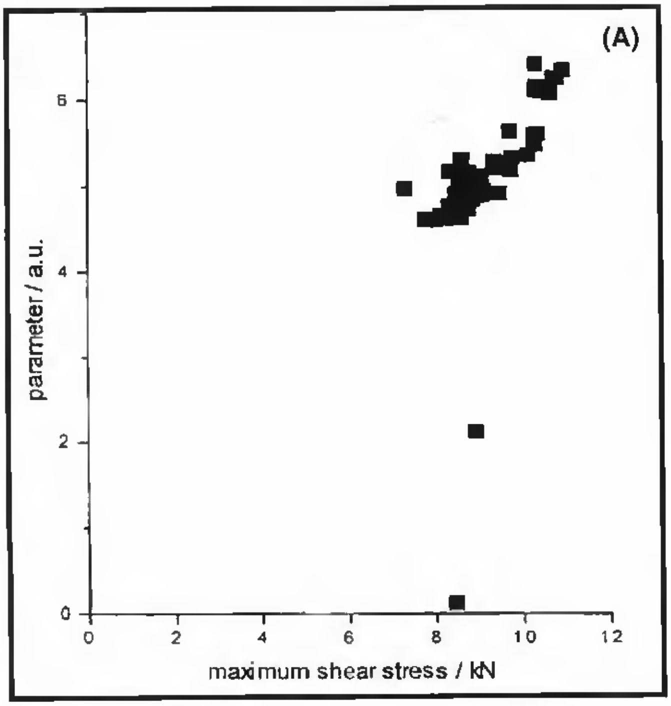

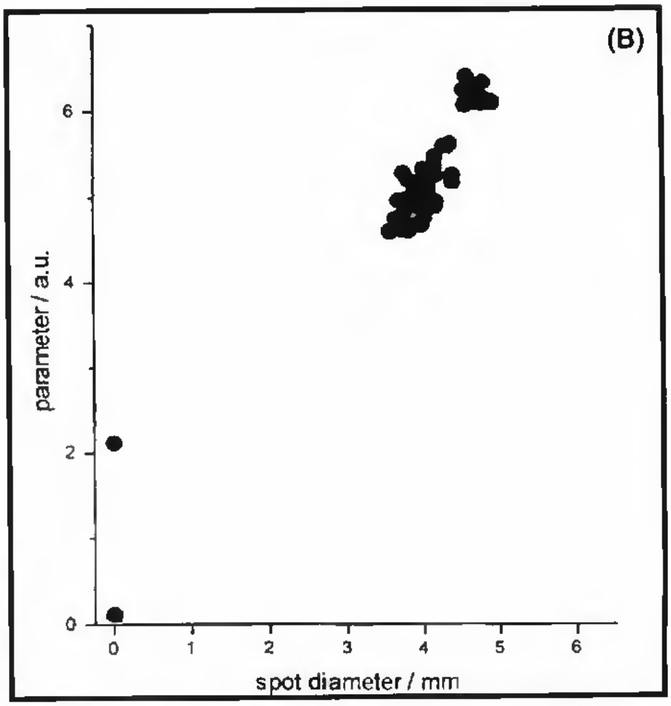

Fig. 5 — Analysis of sensor signal, shear stress and diameter of spot welds. A — Characteristic parameter of spot welds vs. the maximum shear stress; B — characteristic parameter vs. the diameter of the spot welds.

diameter d_a = 5.2 mm and consist of a standard CuCrZr alloy.

As a characteristic parameter for spot welds, the area under the welding peak after subtraction of the plateau value has been chosen, which has the advantage of statistical distortions being averaged out.

A variety of destructive methods have been proposed to define the quality of a spot weld (Ref. 12). To confirm the significance of the sensor signal, a large series of spot welds was performed in which the sensor signals, maximum shear stress and diameter of each spot weld were registered. In Fig. 5A, the sensor signal has been plotted against the maximum shear stress. With only two exceptions, a proportionality between both quantities is apparent. In these cases, although the maximum shear stress is within the range for optimal spot welds, no correct nugget is formed. In Fig. 5B, the diameter of these spot welds was zero. As expected, the characteristic parameter of these welds is comparable with shielded metal arc welds.

Another way to determine the quality of spot welds is to destroy the spot weld by shear stress or torque and measure the diameter of the resulting nugget with Vernier callipers. This method allows determination of the spot diameter with an accuracy of ±0.5 mm, which is sufficient for our purpose.

In Fig. 5B, the same welding parameter as in 5A has been plotted against the diameter of the spot weld (both evaluations have been performed on data corresponding to identical welds). In the second case, the dependence between both quantities is exhibited by less statistical scatter. Determination of the spot diameters by evaluation of the electrode force shows an accuracy of about ±0.7 mm, which can be explained by the inaccuracy in the measurement of the spot weld diameter. Consequently, it would be a straightforward task to define a threshold parameter characterizing a spot weld that is just acceptable, and thus to realize on-line control of the spot welding process.

In actual practice on the production line, several effects may be present that are superimposed onto the sensor signal during the welding time, which make this procedure impossible.

On the other hand, these effects can be identified. Thus, the sensor system offers the possibility of increasing process reliability through the inspection of the electrode force curves. In the following section these, effects are discussed and possible means to circumvent them are presented.

Measurements in the Production Line

As noted in the previous sections, the sensor allows visualization of the electrode arm deflection over the whole welding process. In this context, deviations from the optimal timing as well as from the correct electrode force can be monitored. Furthermore, effects of unexpected importance in the production line that may have a serious influence on the quality of the spot welds could be identified.

Optimal Parameters for the Welding Process

The visualization of the welding process enables on-line control of the welding parameters that has not yet been possible in the production line.

The optimal squeeze time, and particularly the hold time, can be determined and controlled over long periods of time. The optimal beginning of welding can be evaluated by means of the electrode force curves. It is generally accepted that the welding current should not be initiated before 90% of the necessary electrode force is attained. In practice we have found that, in nearly all cases, welding begins either too early or too late. Figure 6 shows two electrode force curves measured in the production line with a squeeze time that is too short (Fig. 6A) and to long — Fig.6B.

In many cases, a considerable reduction of the hold time is possible. A rough estimate shows that a rigorous decrease of the hold time toward its minimum results in a time savings of about five min in the production of a car body. The economic benefits of this procedure are obvious.

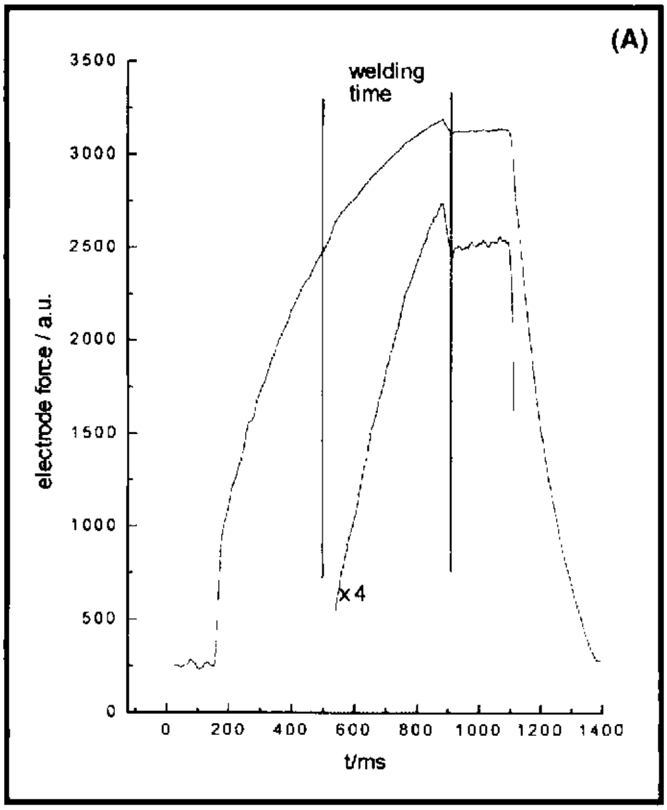

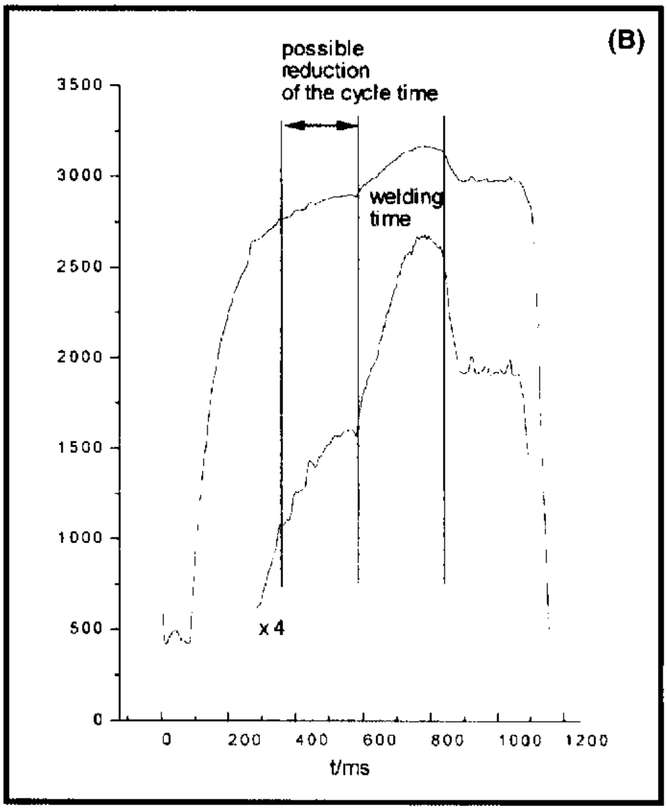

Fig. 6 — Electrode force curve measured in the production line: A — with too short squeeze time; B — with too long squeeze time.

On the other hand, it has been observed that welding starts before sufficient electrode force is reached. The direct influence of too low an electrode force on the quality of the spot weld has not been systematically examined, but it is observed that low electrode forces cause an increased rate of spattering. Generally, spatters are considered as spot welds of sufficient mechanical strength but they exhibit smaller spot diameters than welds produced directly beyond the so-called spatter limit (Ref. 13). Hence, they obviously should be minimized. In this case, an enlargement of the squeeze time or, to minimize the cycle time, the application of special hydraulical mechanisms (so-called power packages) to ensure a fast electrode force buildup, should be taken into account.

Furthermore, the sensor allows the determination of a sufficient hold time. It is necessary that the electrode force is applied to the solidifying nugget to prevent the formation of shrink holes and microcracks (Ref. 14). This is achieved if the hold time ends when the nugget has cooled down, which is indicated by a constant electrode force.

Since there is a linear correspondence between the sensor signal q and the electrode force, the sensor enables us to adjust and to control the electrode force on-line in the production process. Hence, the occurrence of faulty welds caused by too low an electrode force, as well as enhanced wear and tear of the equipment due to too large an electrode force, can be avoided.

Distortions Caused by Adjacent Robots

Signal curves measured in the production line where several robots are working simultaneously on the same workpiece often exhibit features that indicate a change in electrode force up to 400 N — Fig. 7. These features were interpreted as mechanical coupling caused when another welding gun is applied to the workpiece during the welding process of the gun under consideration. Since the electrode force may change by more than 10% due to this effect, it seems possible that a movement of the workpiece may cause defects in the solidifying nugget.

Therefore, to circumvent this changing, the robot program was proposed to avoid application of another welding gun as long as one robot is welding.

Mechanical Deficiencies of the Welding Equipment

In practically all cases, a small movement of the tongs can be observed just at the beginning of welding. In this context, two phenomena have been identified: the stick-slip effect of the piston and the sliding effect of the electrode caps that generally superimpose each other.

Stick-Slip Effect of the Piston

This process is distinctly observed in welding guns with a worn cylinder. In Fig. 8A, a sudden increase of the electrode force at the beginning of the welding time can be seen, as well as a remnant height of the electrode force after welding. Neither effect can be explained by the thermal expansion of the nugget during welding alone.

The movement of the piston in the worn cylinder may remain constant due to static friction before the buildup of the electrode force has reached its demanded final value. During the welding time, a periodic magnetic force is applied to the system that leads to a slipping of the piston and, consequently, to an additional buildup of the electrode force (stick-slip effect). For standard welding equipment, this magnetic force is estimated at 10 N, which is less than 1% of the complete electrode force buildup and is hardly visible in the sensor signals at the low magnification as presented here. Nevertheless, this can give rise to a release of static friction.

As has been observed, the height of

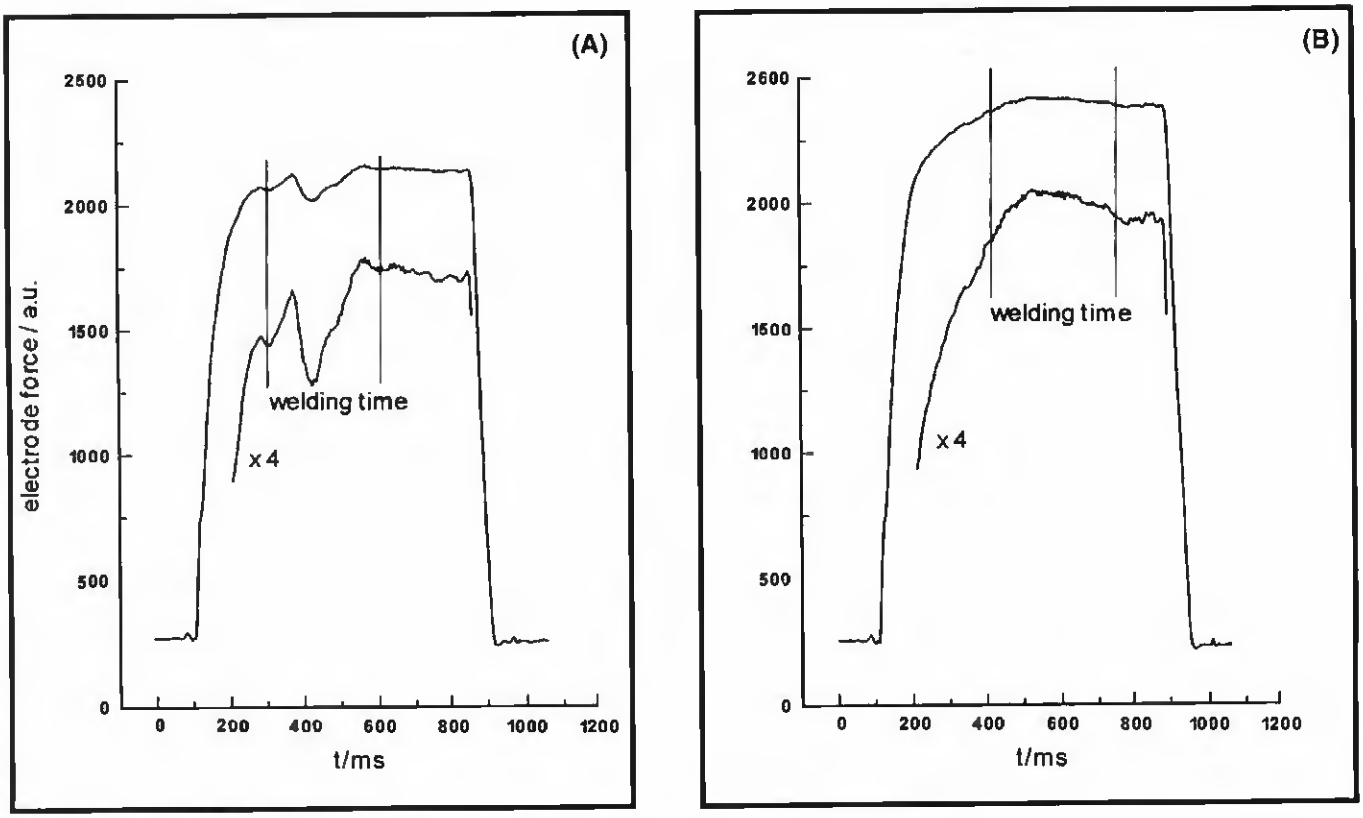

Fig. 7 — Electrode force curves: A — of a weld disturbed by an adjacent robot; B — after avoiding the perturbation.

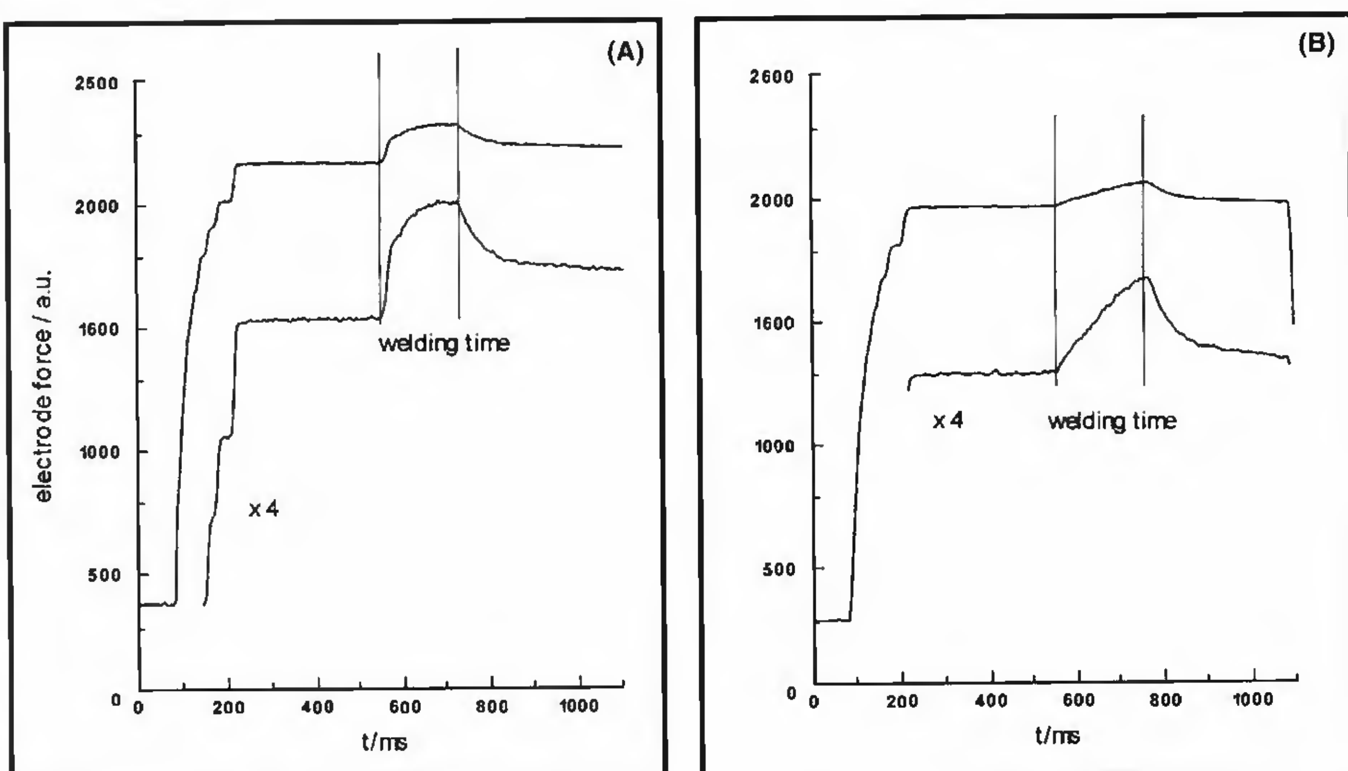

Fig. 8 — A — Electrode force curve of welding tongs with stick-slip effect; B — electrode force curve of the same welding gun after fixing the piston at the end of the electrode force buildup.

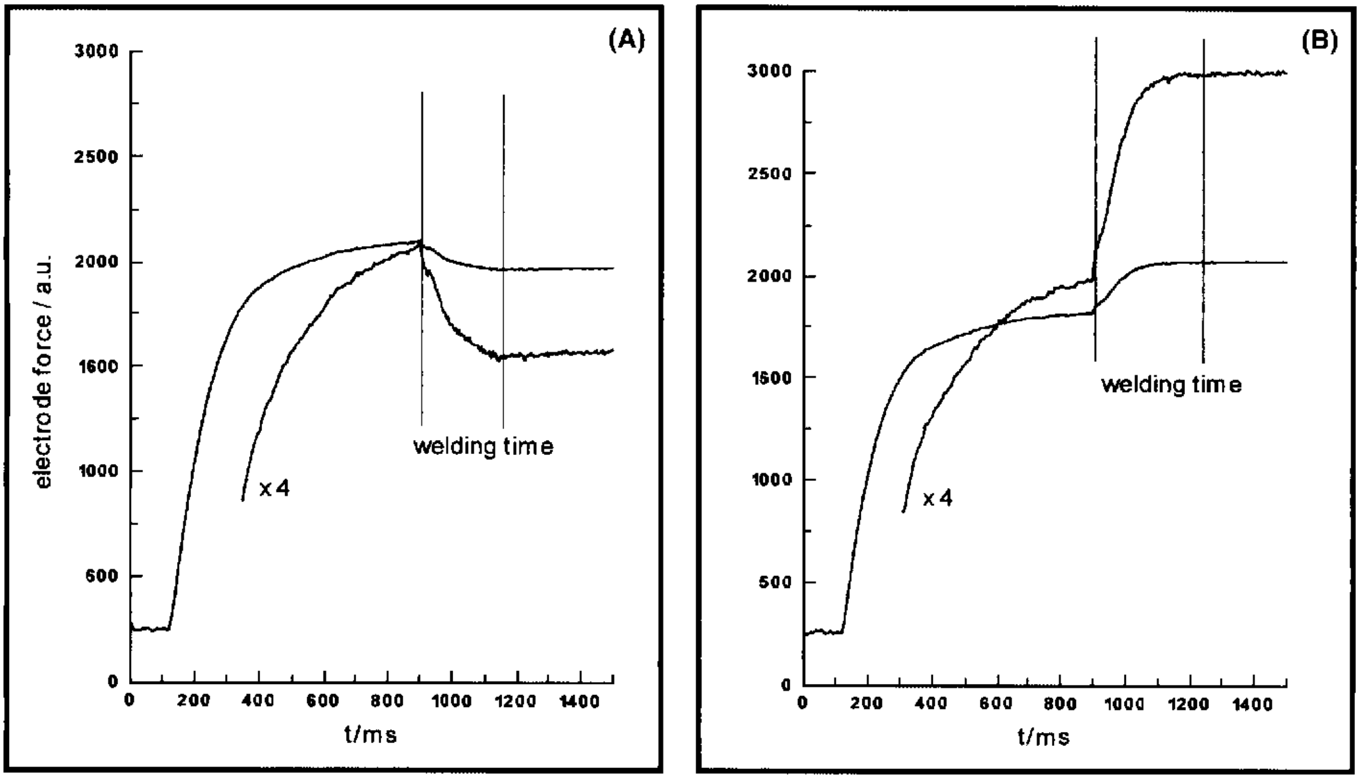

Fig. 9 — Electrode force curves of a welding gun with sliding electrode caps. A — Sensor application at the electrode arm that moves backward; B — sensor mounted at the electrode arm that moves forward.

the sudden increase is not reproducible. Therefore, the quality of the resulting joints cannot be expected to be uniform. Particularly for welding equipment with a highly worn cylinder-piston system, the additional electrode force buildup can exceed 10% and faulty welding cannot be excluded.

To avoid the difficulties caused by the stick-slip effect, the following is proposed:

1) Fix the piston after the electrode force buildup with a clamping device applied at the welding gun or pressure applied to the piston side of the cylinder.

2) Initiate the stick-slip effect with short current impulse of about two periods (40 ms) just before welding.

It is also possible to correct the sensor signal numerically with the data obtained from an additional sensor that detects the piston movement.

Slide Effect of the Electrode Caps

Another effect, observed on the sensor signals at the beginning of the welding time, is sliding of the electrode caps along the surface of the metal sheets. When the welding gun grasps the workpiece, the motion of the electrode caps on the fixed workpiece is inhibited by friction. During welding, the material between the caps becomes ductile and the caps move.

Strictly speaking, this effect is a rotational motion. Although the torque $|T| = |F_{el} \times L_0|$ applied to the electrode arm by the piston remains constant over the welding process, the electrode force changes due to the movement mentioned above. A small movement forward by δL increases the total length of the lever arm and decreases the electrode force by

$$\delta F_{el} = -F_{el} \cdot \frac{\delta L}{L_0}. \qquad (6)$$

Insetting Equation 6 in Equation 1 shows that the sliding in a forward direction yields an additional deflection of the electrode arm at the position of the sensor, though the electrode force decreases. Consequently, an increasing sensor signal is recognized at the beginning of the welding time. Conversely, a backward movement leads to an increasing electrode force and a decreasing sensor signal — Fig. 9.

A motion of the electrode caps of half a spot diameter during welding may cause serious problems. As the position of the electrode caps changes, the current is not applied to the same position and the Joulean heat is introduced in a larger volume than intended. In the worst case, no nugget is formed or a small ellipsoidal nugget is produced. In the latter case, after the weld time, the electrode force will act only on a small portion of the nugget. According to the outlines of the DVS (Ref. 14), this effect can cause shrink holes and microcracks to occur in the nugget and result in a reduced maximum load capacity.

In addition, it has been observed in many cases that sliding of the caps causes a deformation of the metal sheets in the production line because the surrounding material is made ductile due to the heat generated at the spot weld. This effect should generally be prevented.

The sliding effect can be easily minimized by the use of electrode arms of sufficiently high stiffness. It was observed that the misalignment problem appeared especially in spot welding machines of the rocker-arm type with long electrode arms. The adjustment of the electrode arms at press-type welding tongs is easier and it may be considered that misalignment caused by wear develops slower due to the different type of bearings used in their setup.

Conclusion and Outlook

The proposed sensor system offers several possibilities: visualization and optimization of the welding process, online observation in the production line and a comprehensive analysis of the welding equipment, in contrast to other systems that cannot be implemented for geometrical reasons or due to problems in the measurement technique. In this context, the sensor allows the study of a multitude of effects that accompany resistance spot welding. The visualization and control of the process timing and electrode force buildup before welding is especially easy.

Although it has been possible to observe a variety of important quantities in resistance spot welding for a long time, the influence of the mechanical deficiencies of the equipment, in particular, should be more carefully considered. The stick-slip effect of the piston leads to changing welding conditions and the sliding effect of the electrode caps may cause bad welds.

Skeptics maintain that correct welding makes a control system superfluous. This would be correct only if the welding equipment did not display the above-mentioned defects. Consequently, proper welding requires monitoring and control. This sensor is believed to be a well-suited tool for this purpose.

Acknowledgments

The authors wish to thank the following people: W. Schlattl, owner, BT company, initiated development of the sensor system and financially supported the whole project. A. Senk, F. Salzberger and R. Moos carried out many experiments with care and precision. A. Theiler, W. Braumandl and D. Gronemann developed the hardware. I. Bader and P. Salomon developed the system software. Pruf. Dr. R. Labusch and Y. Filbrandt proofread and edited the text.

References

1. Gould, E. 1987. An examination of nugget development during spot welding using both experimental and analytical techniques. *Welding Journal* 65(1): 1-s to 9-s.

2. Greitmann, M. 1993. Quality assurance by numerical analysis of mechanical and thermal processes during resistance spot welding. Conclusive report. MPA, Stuttgart, Germany.

3. Quanz, F. 1994. Process analysis at resistance spot welding of metal sheets coated with zinc on both sides. Ph.D. thesis. TU, Berlin, Germany.

4. Weber, G., and Press, H. 1993. Dynamical current — voltage characteristics at resistance spot welding. Schweißen und Schneiden 45: 153–156.

Weber, G., and Press, H. 1993. The current dependency of the work piece resistance at resistance spot welding with alternating current. Schweißen und Schneiden 45: 32–36.

5. Weber, G., Burmeister, J., and Press, H. 1994. Fuzzy classification — a method for quality evaluation at resistance spot welding. *DVS-Berichte* 165: 70–75.

6. Dorn, L., Habenicht, G., Leichtle, K., Quanz, A., and Wanke, R. 1993. Contribution for quality assurance at resistance spot welding of metal sheets coated with zinc on both sides in the automotive industry. *DVS-Berichte* 143: 121–127.

7. Stiebel, A., Ulmer, C., Kodrack, D., and Holmes, B. 8. 1986. Monitoring and Control of Spot Weld Operations. SAE Technical Paper Series No. 850579.

8. Satonaga, S., and Tatsukawa, I. 1990. Ultrasonic measurements of resistance spot welds by imaging. *Welding International* 4: 813–818. Translation from *Welding Technique* 3: 60–65.

9. Hain, R. 1988. Resistance testing of spot welds challenges ultrasonics. *Welding Journal* 67(5): 46–50.

10. Polrolniczak, H. 1995. Nondestructive evaluation, surveillance and control as a tool for quality assurance at resistance spot welding. *DVS-Berichte* 165: 54–69.

11. Tsai, C. L., Dai, W. L., Dickinson, D. W., and Papritan, J. C. 1991. Analysis and development of a real-time control methodology in resistance spot welding. *Welding Journal* 70(12): 339-s to 351-s.

12. Dorn, L., and Xu, P. 1988. Influence of the mechanical properties of resistance spot welding machines on the quality at resistance spot welding. Schweißen und Schneiden 45: 9–14.

13. Lohbrand, H., and Frings, A. 1989. Resistance spot welding of steel metal sheets coated with zinc. *Thyssen Technische Berichte*, H.2: 213–220.

14. Deutscher Verband für Schweißtechnik e.V. (DVS, Publischer) 1993. *Resistance Spot Welding of Steel Metal Sheets up to a Thickness of 3 mm.* DVS-Verlag, Düsseldorf, Germany.